JET-STUDIES AND α_s-DETERMINATIONS AT HERA

G.W. BUSCHHORN

Max-Planck-Institut für Physik (Werner-Heisenberg-Institut)
(Föhringer Ring 6, 80805 München)

UDC 621.1

Recent results from the H1 and ZEUS collaborations on inclusive single and multiple jet productions in neutral current deep inelastic scattering of electrons/positrons on protons and high energy photoproduction on protons at HERA are reported. The procedures for jet analysis are briefly described and the experimental results are compared with NLO QCD calculations. Determinations of the strong interaction coupling constant α_s from these jet measurements are discussed.

Introduction

The study of jets in deep inelastic scattering (DIS) of electrons/positrons on protons and high energy photoproduction (HEP) on protons enables sensitive tests of QCD in NLO and provides precision measurements of the strong interaction coupling constant α_s. In this report, a survey is given on results from recent measurements of jet production in neutral current processes from the H1 and the ZEUS collaborations at the HERA collider; not included in this review are jets associated with diffraction, heavy flavours or direct photons.

In jet studies, QCD predictions for DIS and HEP are probed in different regions of the DIS variables (Bjorken)x and Q^2 (with $y = Q^2/sx$ and s the squared ep-centre-of-mass energy) and the transverse energy E_{T} and pseudorapidity η_j (defined as $\eta_j = -\log \mathrm{tg}\,\Theta_j/2$ with Θ_j the polar jet angle with respect to the parton beam) of the hadronic jet or jets. In DIS, the virtual photon emitted from the electron interacts with a parton from the proton in a direct (pointlike) process while, at low Q^2 and in HEP, the quasi-real photon can fluctuate into partons, such that, in so-called resolved processes, one of those interacts with partons of the proton (Fig. 1).

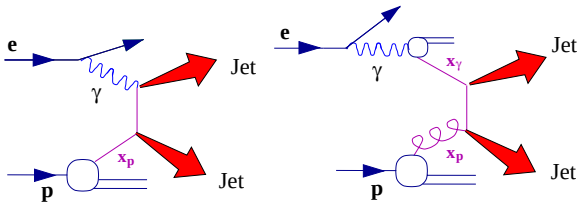

Fig. 1. Examples of leading-order contributions to inclusive jet production: (left) direct photon interaction, (right) resolved photon interaction

In pQCD, jet production depends on the hard partonic scattering process and on the parton density functions (PDFs) of the proton and, in HEP and low Q^2 processes, also of the photon. In DIS (for HEP see Chap. 3), for the calculation of the jet cross section σ_j the hard partonic cross section $d\sigma_a$, is calculated in pQCD for a parton a has to be convoluted (1) with the PDFs f_a of the proton

$$\sigma_j = \sum_a \int dx f_a(x,\mu_F^2) d\sigma_a(x,\alpha_s(\mu_R^2),\mu_R^2,\mu_F^2) \times \times(1+\delta_{\mathrm{hadr}}) \quad (1)$$

and corrected for (nonperturbative) hadronization effects. The dependence of the PDFs on the characteristic scale of the interaction is described by evolution equations, i.e. for not too small x and Q^2, by the DGLAP equations. The summed up higher order contributions of this evolution, corresponding to multiple collinear gluon emissions of the interacting parton, are represented by parton cascade diagrams. Examples of LO contributions to DIS are shown in Fig. 2. According to the factorization theorem, the soft (nonperturbative) part of these corrections can be absorbed in the PDFs while the hard part has to be accounted for in the perturbative part of the interaction, giving the factorization scale μ_F. A breakdown of the DGLAP approximation is to be expected in the small x region, where $\log 1/x$-terms are dominating over $\log Q^2$-terms; in this region, the BFKL evolution equation should give a better description of DIS. A kind of interpolation between these approximations is provided by the CCFM approach.

A preferred reference system for analyzing jet processes in DIS is the Breit (brick wall) system in which the parton collides head-on with the timelike virtual photon: $2x\boldsymbol{p}+\boldsymbol{q}=0$. In the quark parton model (QPM), the hadron jet resulting from the backscattered quark (the Born term) is produced collinear with the proton

remnants, i.e. in the forward direction with respect to the proton beam, whereas hard processes in QCD are characterized by jets with high transverse momenta with respect to the proton remnants. Analyzing the hadronic final state in the Breit system therefore suppresses the QPM background.

The identification of jets within the many hadrons contained in the final state of high energy collider experiments is achieved by algorithms which are applied to the objects of the measurement, i.e. the particle tracks and energy clusters that are registered by the detector. Different jet algorithms have been developed and applied to HERA experiments, but, in recent years, the "inclusive longitudinally invariant k_{T} cluster algorithm" (in the following: ILICA) has emerged as the preferred one. In this algorithm, the objects (particles) are clustered into pairs in an iterative procedure, in which a distance measure $d_{i,j}$ for a particle pair i,j and d_i for a particle i serves as ordering variable:

$$d_{ij} = \min(E^2_{\mathrm{T},i}, E^2_{\mathrm{T},j})(\Delta\eta^2_{i,j} + \Delta\phi^2_{i,j}),$$
$$d_i = E^2_{\mathrm{T},i};\ \text{(distance parameter } R = 1). \qquad (2)$$

Here, $E_{\mathrm{T},i}$ is the transverse energy of a particle i and $\Delta\eta_{ij}$ resp. $\Delta\phi_{ij}$ are the differences in the pseudorapidity η resp. azimuthal angle ϕ of i,j; all these quantities are invariant under longitudinal boosts, i.e. in the direction of the proton beam (defined as $+z$-direction). The algorithm is infrared and collinear safe, can be applied to measurements of DIS and HEP processes. It has been found to typically have the smallest hadronization corrections when compared to other clustering algorithms.

In order to provide reliable tests of QCD, the measured jet cross sections have to be compared with calculations performed (at least) to NLO. These programs yield partonic final states and, therefore, have to be combined with models for the development of the parton cascade and the hadronization. Models used for the development of the parton cascade are the parton shower model, implemented in HERWIG and LEPTO, and the dipole cascade model, implemented in ARIADNE. The hadronization of the partons is modelled by the cluster model, implemented in HERWIG, or by the string fragmentation model, implemented in JETSET and used in LEPTO and ARIADNE. As in LEPTO, in RAPGAP, the LO QCD matrix elements are matched to DGLAP based parton showers in LL approximation. RAPGAP, besides simulating direct processes, allows one to simulate

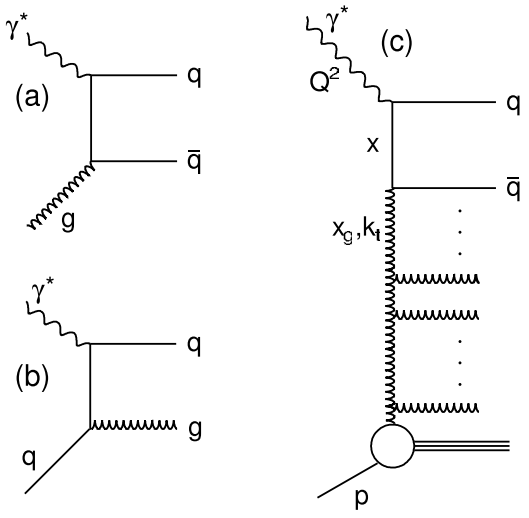

Fig. 2. Leading order diagrams for dijet production: (a) photon-gluon fusion; (b) QCD-Compton process; (c) parton cascade

resolved photon processes in addition. In CASCADE, the QCD matrix elements are combined with parton emission described by CCFM evolution with unintegrated gluon densitiy distribution used as input.

In HEP, direct and resolved interactions are simulated with PYTHIA, HERWIG, and PHOJET. In these programs, the hard partonic interaction in LO is described by QCD matrix elements and the parton cascade is simulated by initial and final state parton showers in LL approximation. In PYTHIA and PHOJET, the hadronization is simulated with the Lund string model as implemented in JETSET; in HERWIG, the cluster model is used.

For the PDFs of the proton, commonly used parametrizations are different versions of CTEQ and MRST, while, for the photon PDFs, GRV and AFG are used.

In the following, we refer for details on the H1 and ZEUS detector and QCD calculations, detector simulations, PDFs to the original papers.

1. Jets in Deep Inelastic Scattering

Results on inclusive jet production have been obtained on single jets, dijets, and trijets and recently also on subjets. Since jet production at small x in the forward direction is closely related to corresponding single hadron production, also such results on π°-production are discussed.

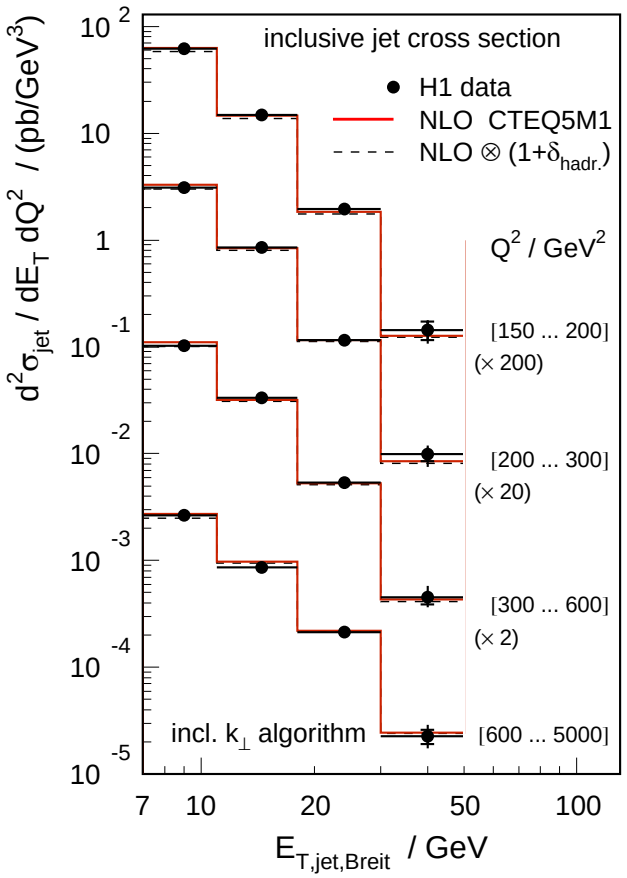

Fig. 3. Inclusive jet cross section in DIS as function of the transverse jet energy in the Breit system $E_{\mathrm{T}jB}$ for regions of Q^2

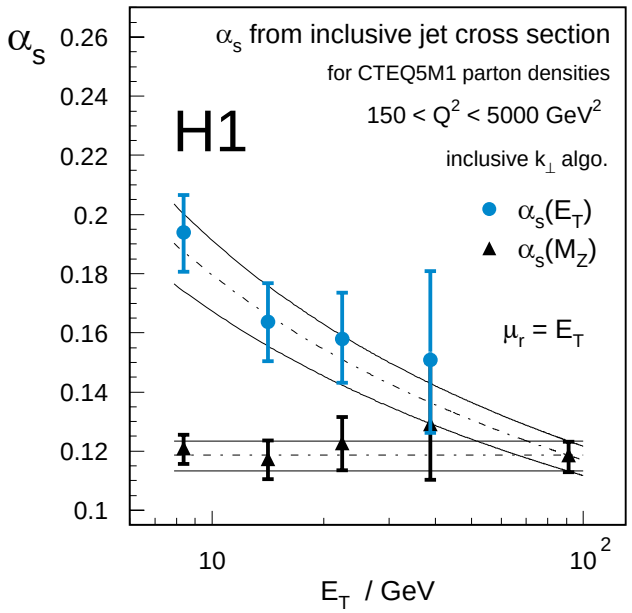

Fig. 4. α_s-determination from inclusive jet cross sections in DIS: Results on $\alpha_s(E_{\mathrm{T}})$ (dots) with fits showing the energy dependence predicted by the renormalization group equation; results extrapolated to $\alpha_s(M_Z)$ (triangles) with combined fit including errors and the combined result on $\alpha_s(M_Z)$ (rightmost triangle)

1.1. Inclusive Jets

At high Q^2, i.e. for $150 < Q^2 < 5000\,\mathrm{GeV}^2$, the inclusive jet cross section has been measured by H1 [1] in the Breit frame as a function of the jet transverse energy E_{T} for $7 < E_{\mathrm{T}} < 50$ GeV^2, $0.2 < y < 0.6$ and $-1 < \eta_{\mathrm{lab}} < 2.5$. Jets have been identified using ILICA. Over the whole range of E_{T} and Q^2, the NLO calculation corrected for hadronization effects ($< 10\%$), gives a good description of the data (Fig. 3).

Fitting the QCD prediction to these cross sections using CTEQ5M1, $\mu_R = E_{\mathrm{T}}$ and $\mu_F = \sqrt{200\,\mathrm{GeV}^2}$ (the average E_{T} of the jet sample) as input yields α_s. First, in separate fits to the data points in the four Q^2 regions, $\alpha_s(E_{\mathrm{T}})$ was determined and evolved to $\alpha_s(M_Z)$. The consistency of these separate fits among each other and with the E_{T}-dependence expected from the renormalization group equation therefore justifies a combined fit to all data points (Fig. 4). The final result, taking into account uncertainties of the renormalization scale ($\mu_R = E_{Tj}$) and from the parton parametrization, is $\alpha_s(M_Z) = 0.1186 + / - 0.0030(\mathrm{exp}) + 0.0039/ - 0.0045(\mathrm{theor}) + 0.0033/ - 0.0023$ (PDF). The experimental error is dominated by the hadronic energy scale of the LAr calorimeter with the statistical error contributing only 0.0007; the theoretical uncertainty includes about equal contributions from the estimate of hadronization and renormalization scale dependence. The result has been shown to be stable against variations of the jet algorithm.

Similar measurements have been performed recently by ZEUS [2] in the Breit system using ILICA. For $Q^2 > 125$ GeV^2, $E_{\mathrm{T}B} > 8$ GeV, pseudorapidites $-2 < \eta_{jB} < 1.8$ and demanding for the angle γ of the hadronic system $-0.7 < \cos_\gamma < 0.5$, the Q^2- and $E_{\mathrm{T}B}$-dependence of the inclusive jet cross section also is found to be in good agreement with NLO QCD calculations.

For the determination of α_s, the differential cross sections $d\sigma/dV$, where $V = Q^2, E_{\mathrm{T}Bj}$, were calculated in NLO QCD for three MRST99 sets, i.e. central, α_s ↑↑ and α_s ↓↓, taking the $\alpha_s(M_Z)$ of the corresponding PDFs for the partonic cross sections. For each bin i in V, the calculated cross sections were parametrized according to $[d\sigma(\alpha_s(M_Z))/dV]_i = C_{1,i}\cdot\alpha_s(M_Z) + C_{2,i}\cdot\alpha_s^2(M_Z)$. From a χ^2 fit to this ansatz, α_s was determined for several regions of V. The best fit ($\chi^2 = 2.1$ for 4 data points)

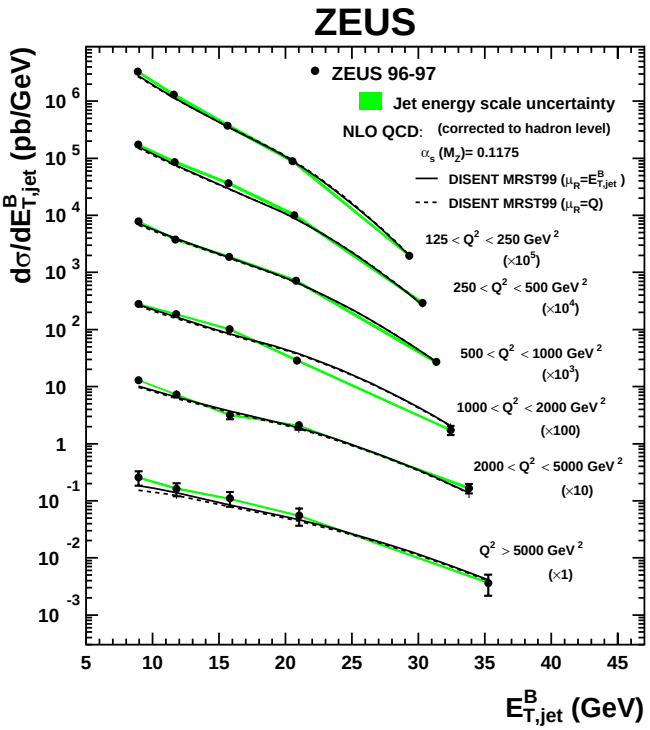

Fig. 5. Inclusive jet cross section in DIS as function of the transverse jet energy in the Breit system $E_{\mathrm{T}jB}$ for different regions of Q^2

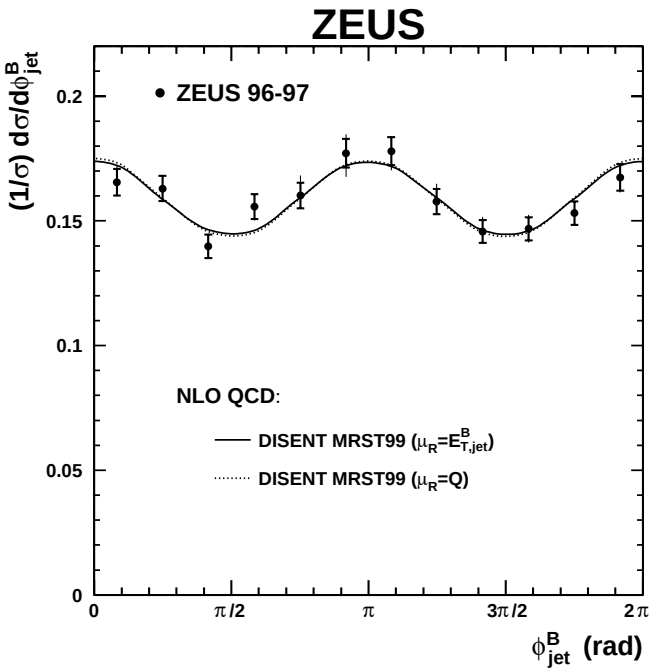

Fig. 6. Normalized differential cross section for inclusive jet production in DIS with $E_{\mathrm{T}B_j} > 8$ GeV and $-2 < \eta_{B_j} < 1.8$; inner errors for statistical, outer errors for combined statistical and systematic errors

was achieved for $Q^2 > 500$ GeV^2 resulting in $\alpha_s(M_Z) = 0.1212 + / - 0.0017$ (stat) $+0.0023/-0.0031$ (syst) $+0.0028/-0.0027$ (theor).

The energy scale dependence of α_s has been investigated using the same procedure but parametrizing the measured cross section in terms of $\alpha_s(\langle E^B_{\mathrm{T_{jet}}}\rangle)$, where $\langle E^B_{\mathrm{T_{jet}}}\rangle$ is the mean value of $E^B_{\mathrm{T_{jet}}}$ in each bin; $\mu_R = E^B_{\mathrm{T_{jet}}}$ was chosen here since it provides the better despription of these data. Good agreement with the predicted running of α_s is found over a large range of $E^B_{\mathrm{T_{jet}}}$ as shown in Fig. 23.

These data have also been used to study the azimuthal distribution of jets in the Breit frame [3]. At LO, the dependence of the cross section on the angle ϕ^B_j between the lepton scattering plane and jets produced with high E_{T} takes the form

$$\frac{d\sigma}{d\phi^B_j} = A + B\cos\phi^B_j + C\cos 2\phi^B_j \qquad (3)$$

where the coefficients A, B, C result from the convolution of the matrix elements for the partonic processes with the PDFs of the proton. The $\cos\phi$-term arises from the interference between transverse and longitudinal components of the exchanged photon (for $Q^2 \ll M_Z^2$), whereas the $\cos 2\phi$-term results from the interference of $+1/-1$-helicity amplitudes of its transversely polarized part; nonperturbative contributions arising from intrinsic transverse momenta of the partons have shown to be small and, therefore, are negligible at high E_{T}. The measured normalized azimuthal distribution shown in Fig. 6 is well reproduced by NLO calculations with either $\mu_R = E_{\mathrm{T}}$ or Q. In view of the small theoretical uncertainties, these measurements constitute a precision test of NLO QCD.

H1 has extended the inclusive jet measurements, also in the Breit frame, to low Q^2 of $5 < Q^2 < 100$ GeV^2 for $0.2 < y < 0.6$, $E_{\mathrm{T}} > 5$ GeV and $-1 < \eta_{\mathrm{lab}} < 2.8$ [4]. The differential cross section as function of E_{T} is shown in Fig. 7 for three bins of η. The good agreement with NLO QCD predictions (for $\mu_R = E_{\mathrm{T}}$) found for the backward and central region, worsens in the forward region of $\eta > 1.5$ and for $E_{\mathrm{T}} < 20$ GeV, where NLO corrections and uncertainties are large. For most of the data, the theoretical uncertainties (given by the renormalization uncertainty) are larger that the experimental errors. Investigating the Q^2 dependence of this discrepancy, it was found to set in for $Q^2 < 20$ GeV^2, indicating that NLO QCD works reasonably well even in the forward region $\eta_{\mathrm{lab}} > 1.5$ as long as both E_{T} and Q^2 are not too small.

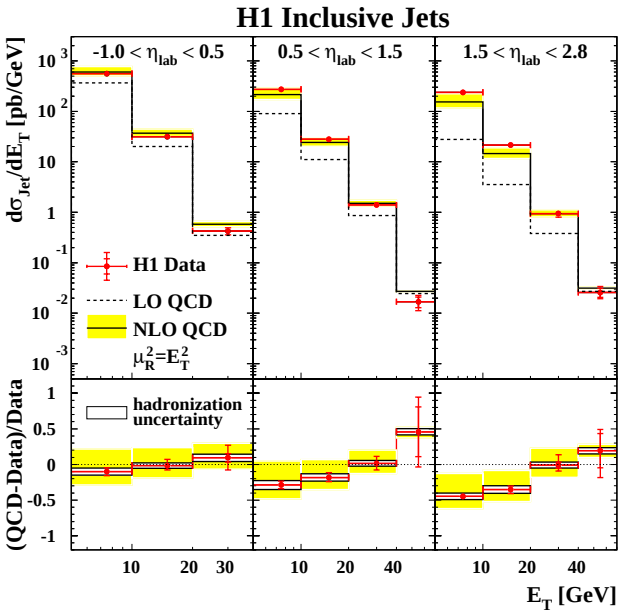

Fig. 7. Inclusive jet cross section $d\sigma/dE_{\rm T}$ in DIS integrated over $5 < Q^2 < 100$ GeV^2 and $0.2 < \eta_y < 0.6$ as function of the transverse jet energy $E_{\rm T}$ in the Breit system for different ranges of $\eta_{\rm lab}$: forward (proton direction): $1.5 < \eta < 2.8$; central: $0.5 < \eta < 1.5$; backward: $-1.0 < \eta < 0.5$. NLO QCD model: DISENT with CTEQ5M (solid line) and no hadronization corrections; hatched band: change of the renormalization scale by 1/2 and 2

In the forward direction, jet production is expected to be sensitive to the dynamics of the parton cascade at small x. It has been suggested by Mueller—Navelet to suppress DGLAP evolution in DIS by demanding of the forward jet $E_{\rm T}^2 \approx Q^2$ while enhancing BFKL evolution by keeping x_j as large as feasible and x/x_j small.

H1 has taken data on inclusive jet production in the forward direction [5], i.e. $7^\circ < \Theta_{j\rm lab} < 20^\circ$ with $0.5 < Q^2/E_{\rm T}^2 < 2$ and $x_j > 0.035$ ($E_{\rm T} > 3.5$ GeV). The measurement and jet search with ILICA are performed in the lab frame with cuts $5 < Q^2 < 75$ GeV^2 and $0.1 < y < 0.7$. The data (Fig. 8) are compared with four different Monte Carlos: RAPGAP, a DGLAP-type MC with direct photon interaction (RG (DIR)), the same MC including a resolved photon component (RG (DIR+RES)), DJANGO which is based on the color dipole model CDM (ARIADNE) and uses random walk transverse momenta similar to BFKL and CASCADE which is an implementation of the CCFM evolution equation. The differential cross sections in x and x_j are up to a factor of two larger than the DGLAP prediction for direct photons only (RG (DIR)), but they are reasonably well described if a resolved photon is included and also by the CDM model; CCFM predicts too large cross sections.

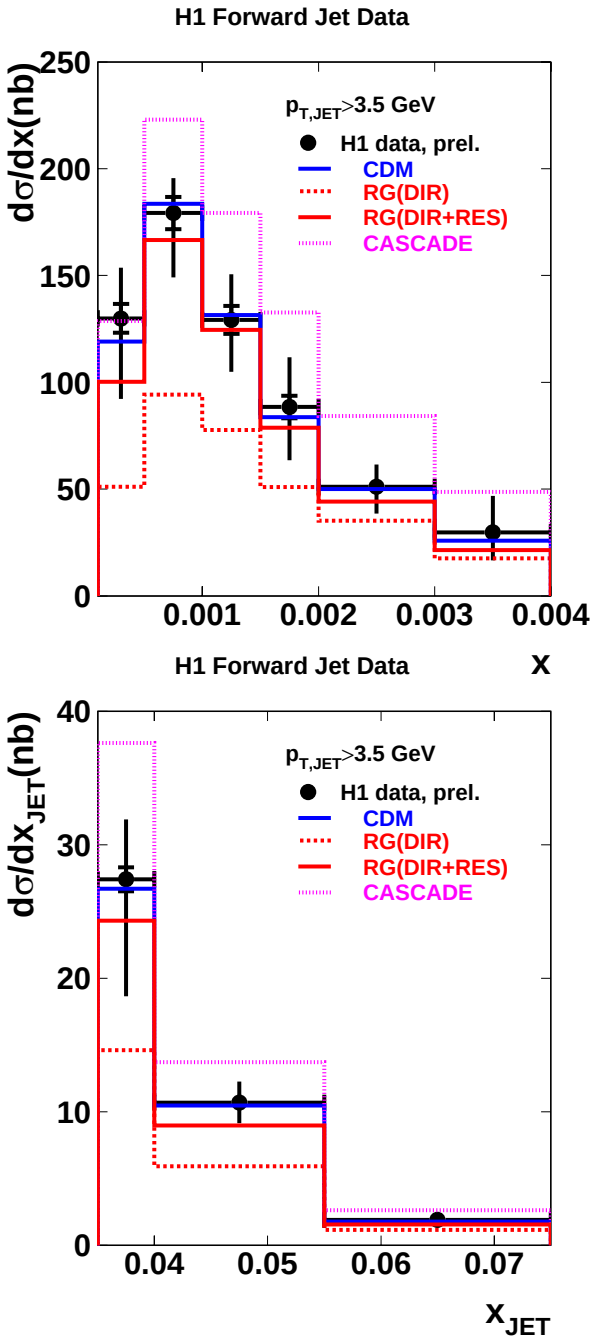

Fig. 8. Inclusive forward jet cross sections in DIS for $p_{{\rm T}j} > 3.5$ GeV; $7^\circ < \Theta_j < 20^\circ$; $x_j > 0.035$ at the hadron level. Models: CDM (Color-Dipole-Model: DJANGO + ARIADNE), RG (RAPGAP: DIRECT and DIRECT + RESOLVED), CASCADE (CCFM). Data are preliminary

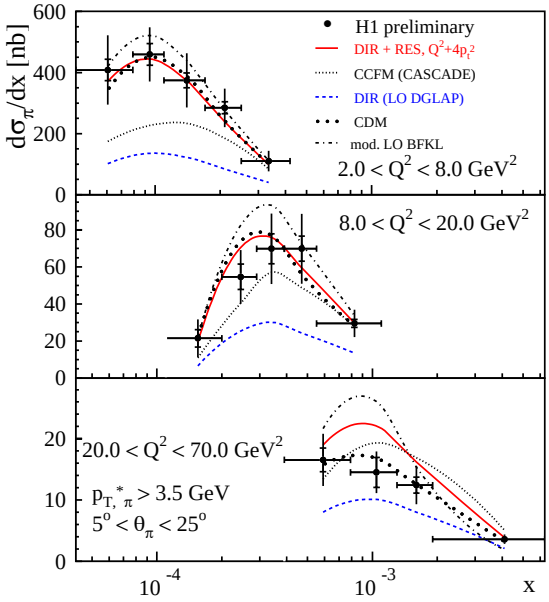

Fig. 9. Inclusive forward π° cross section in DIS for transverse momenta in the γ-proton cms $p^*_{\mathrm{T}\pi^\circ} > 3.5$ GeV and $5^\circ < \Theta\pi^\circ < 25^\circ$ for different ranges of Q^2. Models: DIR (RAPGAP for DIRECT proc.), DIR + RES (RAPGAP for DIRECT + RESOLVED proc.), CCFM (CASCADE), CDM (Color-Dipole-Model: ARIADNE), mod. LO BFKL (modified LO BFKL evolution)

In forward π° production, a forward emitted parton is tagged by a single energetic fragmentation product. While, in principle, in single hadron production smaller forward angles than in jet production can be reached, the cross sections are lower and the hadronization uncertainties are higher.

Inclusive π°-production in DIS has been measured by H1 [6] under slightly different kinematic conditions than in forward jet production with the following cuts: $0.1 < y < 0.6$, $4.10^{-5} < x < 6.10^{-3}$, $2 < Q^2 < 70$ GeV^2 and π° cms-momenta > 2.5 GeV, polar angles of $5^\circ < \Theta_\pi < 25^\circ$ (corresponding to the central region in the hadronic cms) and $x_\pi > 0.01$; no explicit cut on $P^2_{\mathrm{T}\pi^\circ}/Q^2$ was applied. Furthermore, the transverse energy flow was measured which provides a complementary approach to the testing of QCD. In Fig. 9, the differential cross section is compared with QCD-based models. The DGLAP prediction with direct photon interaction only is too low, but the inclusion of resolved photon interaction — albeit with a choice of renormalization and factorization scale $(Q^2 + 4p^2_{\mathrm{T}})$ different from the one in forward jet production $(Q^2+p^2_{\mathrm{T}})$ — yields a good description. While also a BFKL based

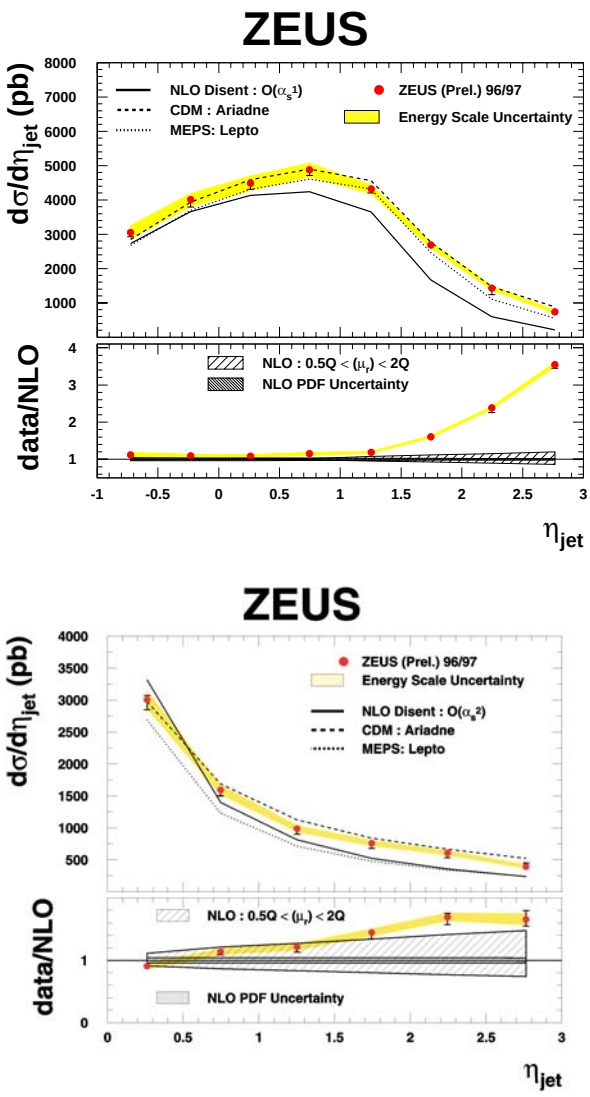

Fig. 10. Upper figure: Inclusive jet cross sections in DIS for $Q^2 > 25$ GeV^2; $y > 0.04$ and $E_{\mathrm{T}j} > 6$ GeV; $-1 < \eta_j < 3$ in comparison to $O(\alpha_s^1)$-NLO QCD calculations in the lab frame ("inclusive phase space", see text). Lower figure: Jet cross sections for the same kinematical conditions but constraining the jet topology to $\eta_j > 0$ and $\cos\gamma_{\mathrm{hadr}} < 0$ in comparison with $O(\alpha_s^2)$-NLO QCD calculations in the lab frame ("dijet phase space")

calculation describes the data reasonably well, CCFM evolution fails at small x.

In a recent measurement jets by ZEUS [7] of inclusive jet production in DIS for $Q^2 > 25$ GeV^2, $y > 0.4$ and with $E_{\mathrm{T}j} > 6$ GeV, $-1 < \eta_j < 3$, deviations of the measured cross section from NLO QCD predictions

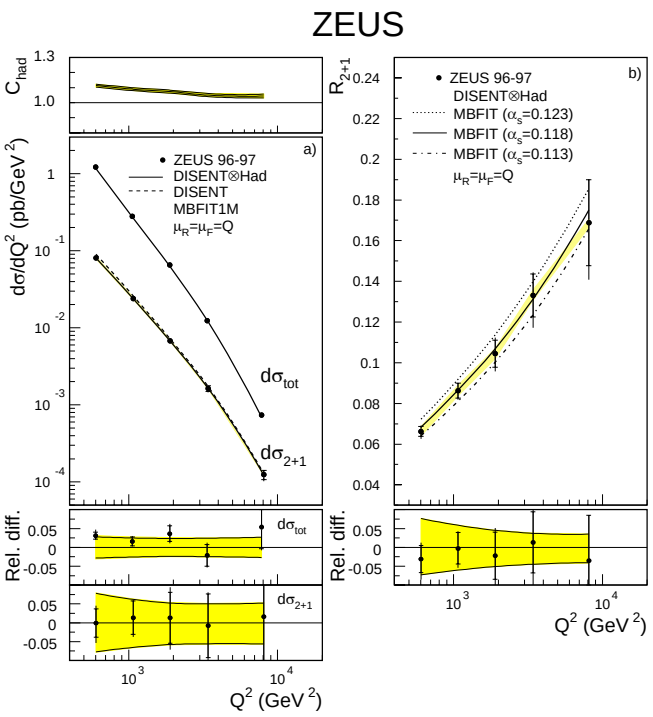

Fig. 11. Inclusive jet ($\sigma_{\rm tot}$) and dijet (σ_{2+1}) cross sections in DIS, hadroniz. corr. C refers to dijets; (right): dijet fraction R_{2+1}, shaded band gives uncertainty due to abs. energy scale of jets

calculated in the lab frame to $O(\alpha_s^1)$ have been stated which strongly increase towards the forward direction (Fig. 10, upper part) and small $E_{{\rm T}j}, Q^2$, and x. In a special analysis of these data, the Mueller-Navelet suggestion (see above) has been applied by combining the detection of a hard forward jet ($E_{{\rm T}j} > 6$ GeV, $0 < \eta_j < 3$) with the requirement that the hadronic angle $\gamma_{\rm hadr}$, corresponding to the direction of the scattered quark in the QPM, is reconstructed in the backward direction of the detector ($\cos\gamma_{\rm hadr} < 0$) thus suppressing QPM contributions to the forward jets. Comparing the cross sections for such defined jet configurations ("dijet phase space") with NLO QCD predictions calculated to $O(\alpha_s^2)$, better agreement (Fig. 10, lower part) is found in the forward direction at the expense of a considerably larger uncertainty in the renormalization scale which swamps a possible BFKL signal in this part of the phase space.

1.2. Dijets

The LO QCD processes which contribute to dijet production in DIS are QCD Compton scattering (QCDC) and boson-gluon-fusion (BGF) (comp. Fig. 2). In the high Q^2 region, where the QCDC process is dominant and the PDFs are well constrained by fits to inclusive DIS data, dijet measurements with α_s as input enable tests of pQCD; at low Q^2, where BGF is dominating, the comparison of measured dijet cross sections with QCD predictions for different PDFs has been used to investigate the gluon distribution.

Dijet measurements in DIS have been performed by H1 [1] and ZEUS [8] in similar kinematic regions with similar analysis methods. To the two jets with the highest $E_{\rm T}$ which are reconstructed with ILICA in the Breit system, asymmetric cuts in $E_{\rm T}$ have to be applied to avoid regions at the boundary of the dijet phase space which are sensitive to soft gluon radiation. The data (Fig. 11) are compared with NLO calculations with DISENT and have been checked with MEPJET. For $O(10\ {\rm GeV}^2) < Q^2 < O(10.000\ {\rm GeV}^2)$ and $E_{{\rm T}B} > 5$ GeV, i.e. when NLO and hadronization corrections are small, the studied jet observables are described within about 10 %; for $Q^2 < 10\ {\rm GeV}^2$, however, where NLO corrections are becoming large, significant disagreement is observed. (For new data on multijet production by ZEUS, see Chap. 2.3.)

From the dijet fraction $R_{2+1}(Q^2)$ measured by ZEUS, α_s was determined using the same method as applied to inclusive jets (Chap. 2.1) with the result $\alpha_s(M_Z) = 0.1166 + / - 0.0019({\rm stat}) + 0.0024/0.0033({\rm exp}) + 0.0057/ - 0.0044({\rm theor})$. The dependence of α_s on the scale Q, which was tested by applying the same fit procedure to $\alpha_s(\overline{Q^2})$, is in good agreement with the expected running of α_s (see Fig. 23).

Recently, the region of low x has been studied in more detail by H1 [9] in the kinematic region $5 < Q^2 < 100\ {\rm GeV}^2$, $10^{-4} < x < 10^{-2}$ and $0.1 < y < 0.7$. For jets reconstructed in the hadronic cms with asymmetric cuts of $E_{\rm T1} > 7$ GeV, $E_{\rm T2} > 5$ GeV within $-1 < \eta < 2.5$, the triple differential dijet cross sections in $(x, Q^2, E_{\rm Tmax})$ (Fig. 12) and $(x, Q^2, \Delta\eta)$ do not show significant deviations from NLO calculations with $\mu_R = (E_{\rm T1} + E_{\rm T2})/2$, $\mu_F = \sqrt{< E_{\rm T}^2 >} = \sqrt{70{\rm GeV}^2}$, in contrast to the ratio of the number of dijet events with azimuthal angle separation of less than 120° to all dijet events (Fig. 13). Better agreement for at least part of the phase space can be achieved by combining LO ME with direct photon processes and k_T ordered parton emission. One would expect calculations based on CCFM evolution, $k_{\rm T}$ factorization or unintegrated gluon density to be better suited to model this kinematical region; comparing the predictions from CASCADE for different choices of unintegrated gluon densities with the

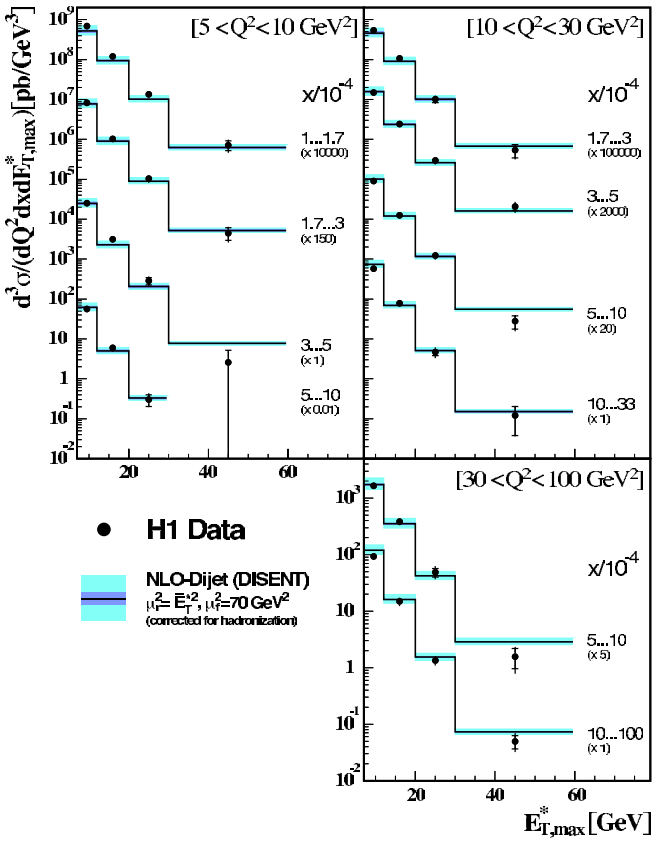

Fig. 12. Inclusive dijet consection in DIS for $10^{-4} < x < 10^{-2}$ as a function of the maximum transverse jet energy E^*_{Tmax} in the hadronic cms compared to NLO QCD predictions using CTEQ5M corrected for hadronization. Outer light error band includes hadronization (dark band) and renorm. scale uncertainties

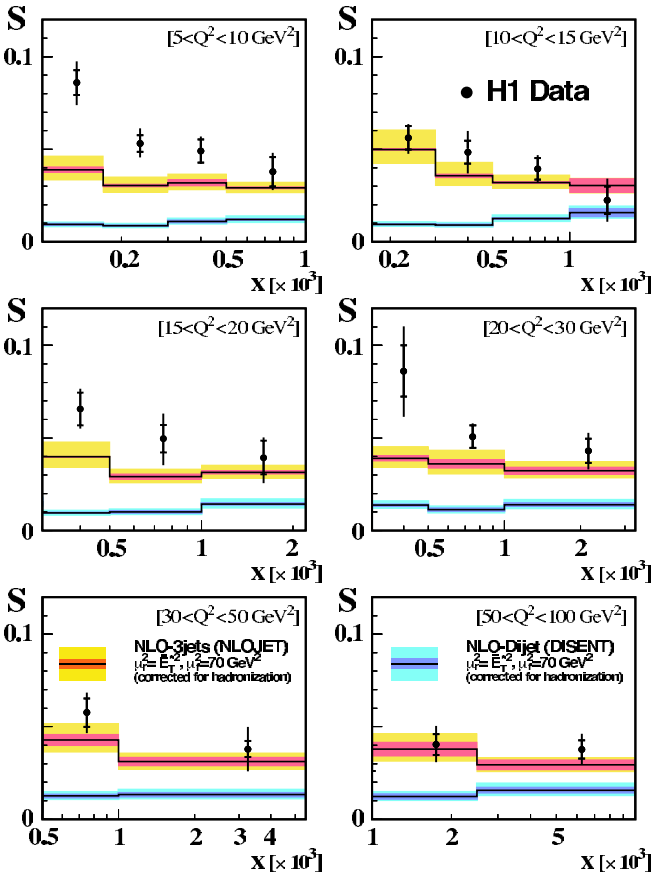

Fig. 13. Ratio S of the number of dijet events with small azimuthal jet separation ($\phi < 2\pi/3$) to the total number of inclusive dijet events as a function of (Bjorken)x compared to NLO QCD predictions and with error bands as in Fig. 12

measurements can provide constraints on the gluon PDF since the NLO uncertainties are usually larger than the data errors.

1.3. Trijets

While the cross sections for inclusive jet and dijet production in LO pQCD depend on $O(\alpha_s)$ only, the trijet cross section already in LO is sensitive to $O(\alpha_s^2)$.

Trijet production in DIS has been measured by H1 [10] for $5 < Q^2 < 5000$ GeV^2, selecting jets with $E_{\mathrm{T}} > 5$ GeV in the Breit frame with ILICA. The measured cross sections (Fig. 14) were compared with LO and NLO calculations using NLOJET with μ_R and μ_F set to the average transverse energy $\overline{E_{\mathrm{T}}}$ of the 3 jets in the Breit frame; for the proton PDFs, CTEQ5M1 was taken with $\alpha_s(M_Z)$ set to 0.118. The inclusive trijet cross sections for invariant masses > 25 GeV as well as the trijet/dijet ratio, in which many theoretical and experimental uncertainties cancel out, in spite of large NLO corrections agree well with the NLO predictions. Also the angular distribution of trijets agrees well with pQCD expectation.

Recent studies of dijet and trijet production by ZEUS [11] for $10 < Q^2 < 5000$ GeV^2 in the kinematic range $0.04 < y < 0.6$, $\cos\gamma_{\mathrm{hadr}} < 0.7$, with cuts $-1 < \eta_{\mathrm{lab}} < 2.5$, $E_{TB} > 5$ GeV defining the jet phase space and with an invariant mass cut of $M_{2j,3j} > 25$ GeV are shown in Figs. 15 and 16. Good agreement is found with the pQCD predictions after correcting for hadronization, i.e. in $O(\alpha_s^3)$.

1.4. Subjet Multiplicities

Reapplication of the jet algorithm with a smaller resolution scale y_{cut} to identified jets is able to resolve

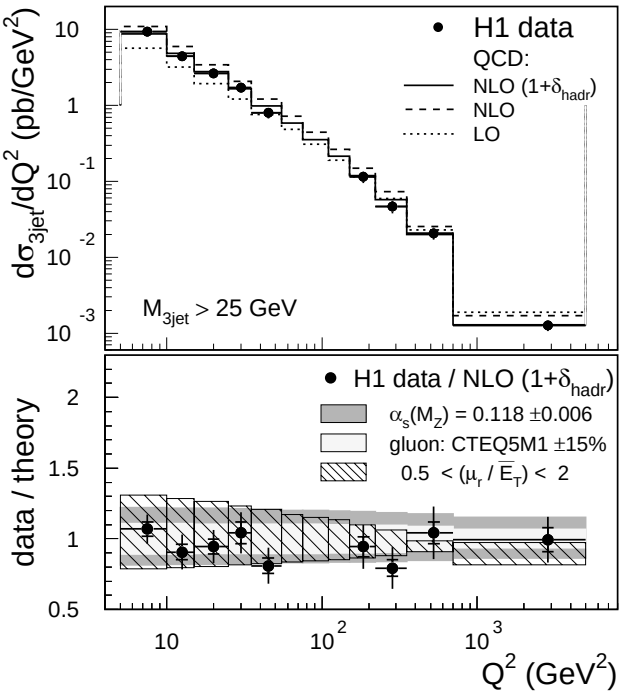

Fig. 14. Inclusive trijet production in DIS for $5 < Q^2 < 5000$ GeV^2; $-1 < \eta_{\rm lab} < 2.5; M_{3j} > 24$ GeV. QCD: NLOJET

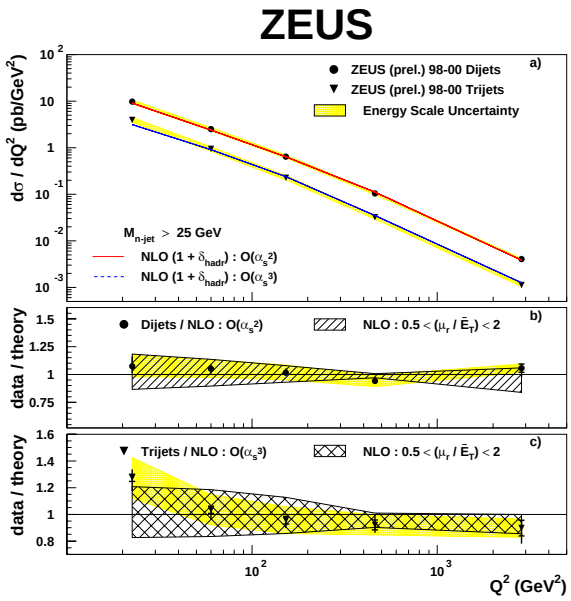

Fig. 15. Inclusive dijet and trijet cross sections in DIS. The light shaded band indicates the calorimeter energy scale uncertainty, the hatched band the renormalization scale uncertainty

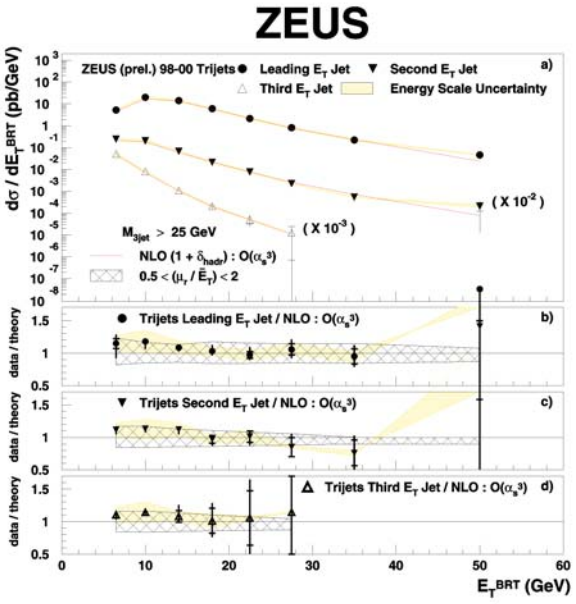

Fig. 16. Inclusive trijet cross section in DIS; error bands as in preceding Fig. 15.

clusters within the jets which are called subjets. In LO, the splitting of a jet into two subjets corresponds to, e.g., the radiation of a gluon by the primary parton. The development of the subjet multiplicity with $y_{\rm cut}$ can be calculated in pQCD for high $E_{{\rm T}j}$ and not too low $y_{\rm cut}$ values, i.e. when fragmentation effects are estimated to be not too large in NLO. Since the subjet multiplicity is mainly determined by QCD radiation in the final state, it only weakly depends on the PDFs of the proton.

The mean subjet multiplicity has been measured by ZEUS [12] in NC DIS processes with $Q^2 > 125$ GeV^2 for $E_{\rm T} > 15$ GeV and $-1 < \eta_j < 2$. ILICA has been applied to jets in the lab frame, where calculations of up to $O(\alpha_s^2)$ can be performed. The mean subjet multiplicity $< n_{sbj} >$ was determined for $5.10^{-4} < y_{\rm cut} < 0.1$. The data are in good agreement with NLO calculations for $\mu_R = \mu_F = Q$ and CTEQ4M PDFs. (Fig. 17).

Using the method described earlier (see Chap. 2.1), α_s was determined from these data yielding for $25 < E_{\rm T} < 71$ GeV and a $y_{\rm cut} = 10^{-2}$, which compromizes between experimental and theoretical errors, a result of $\alpha_s(M_Z) = 0.1187 + / - 0.0017({\rm stat}) + 0.0024/ - 0.0009({\rm syst}) + 0.0093/ - 0.0076({\rm theor})$. While the experimental uncertainty is comparable to the one resulting from jet measurements, the theoretical uncertainty is larger and dominated by NNLO terms.

2. Jets in High Energy Photoproduction

In LO QCD direct as well as resolved processes (comp. Chap. 1) have to be considered in the calculation of the jet cross section. With x_γ as the fractional momentum of the photon-parton and x_p as the fractional momentum of the proton-parton participating in the hard scatter, the jet cross section, therefore, is given as the convolution of the photon PDF $f_{\gamma b}(x_\gamma, \mu^2)$ and proton PDF $f_{pa}(x_p, \mu^2)$ with the hard partonic cross section $d\sigma_{a,b}(x_\gamma, x_p, \mu^2)$

$$\sigma_j = \sum_{a,b} \int\int dx_\gamma dx_p f_{pa}(x_p, \mu^2) f_{\gamma_b}(x_\gamma, \mu^2) \times$$
$$\times d\sigma_{a,b}(x_p, x_\gamma, \mu^2) \cdot (1 + \delta_{\rm hadr}) \qquad (4)$$

summed over all partons a, b from the photon and proton. For direct photon interaction, f_γ equals the δ-function at $x_\gamma = 1$. Since the transverse energy $E_{\rm T}$ of the jet or jet system is the only scale parameter available in jet photoproduction involving light quarks only, μ_R and μ_F are set $\mu_R = \mu_F = \mu = E_{\rm T}$. In resolved processes besides the partons interacting in the hard scatter, photon fragments may interact with proton remnants causing a background of multiparton interactions ("underlying events"), which has to be corrected for but remains below 10% for $E_{\rm T} > 20$ GeV.

In photoproduction of jets at HERA, the proton PDFs are, with the current statistics, predominantly probed by partons in the range of $0.05 < x_p < 0.5$, where they are well constrained by measurements of F_2^p, while the probed range in the photon PDFs is $0.1 < x_\gamma < 1$. While the quarks are well constrained for $x_\gamma < 0.5$ by measurements of F_2^γ at LEP, the gluon is only poorly constrained. HERA offers the advantage that jet production is sensitive to the gluon in the photon already on LO, and in addition it allows the study of the photon structure at higher scales.

Detailed studies on the inclusive photoproduction of jets have been performed on inclusive jets and dijets. In single jet production, in comparison to dijets production, an increased kinematic range is accessible, higher statistical accuracy can be achieved and infrared dangerous regions of phase space are not existent; on the other side, single jet photoproduction is less sensitive to details of the hard scatter process.

2.1. Inclusive Jets

H1 [13] and ZEUS [14] have performed similar measurements and analyses of the inclusive jet cross sections for photons of $Q^2 < 1$ GeV^2 both using ILICA

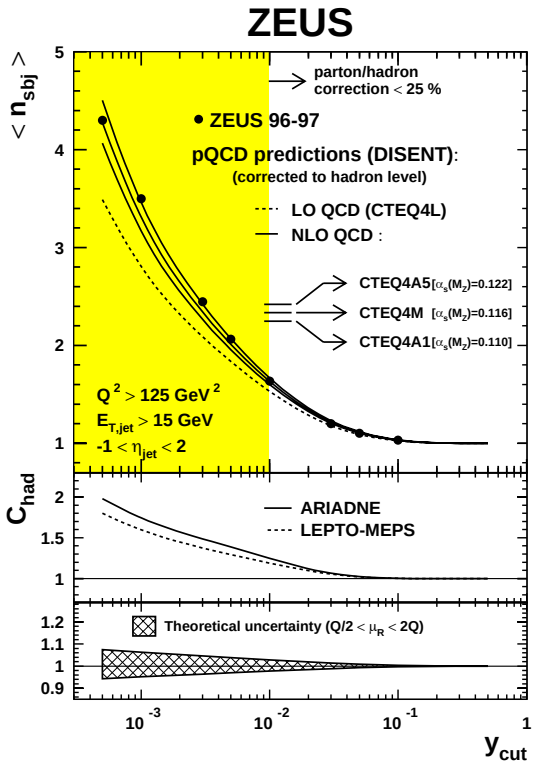

Fig. 17. Mean subjet multiplicity as a function of $y_{\rm cut}$ in inclusive jet production in DIS for $E_{{\rm T}j} > 15$ GeV; $Q^2 > 125$ GeV^2 and $-1 < \eta_j < 2$

for jet reconstruction within $-1 < \eta_j < 2.5$. The H1 data for $E_{\rm T} > 21$ GeV cover a kinematic range of $95 < W_{\gamma p} < 285$ GeV. The measurements were extended to $E_{\rm T} > 5$ GeV with a dedicated trigger for photons of $Q^2 < 0.01$ GeV^2 in the restricted kinematic range of $164 < W_{\gamma p} < 242$ GeV. The ZEUS data were taken for $142 < W_{\gamma p} < 293$ GeV for $E_{\rm T} > 17$ GeV (see Fig. 18). H1 compares the data with the NLO QCD calculations of Frixione and Ridolfi, using CTEQ5M1 for the proton PDFs and GRV for the photon PDFs, setting $\mu_R = \mu_F$ to the average transverse energy of the two outgoing partons; ZEUS compares with Klasen, Kleinwort, Kramer, using MRST99 for the proton and GRV for the photon with $\mu_R = \mu_F = E_{{\rm T}j}$. In both analyses, a good agreement with NLO QCD over six orders of the magnitude of the cross section is found; however, the H1 data for $Q^2 < 0.01$ GeV and $5 < E_{\rm T} < 12$ GeV may indicate a cross section rising above prediction with increasing η.

From the ZEUS data, also $\alpha_s(M_Z)$ was determined (see Chap. 2.1) by calculating in NLO QCD for each $E_{\rm T}$-bin i the cross section $(d\sigma/dE_{\rm T})_i$ using the three sets of

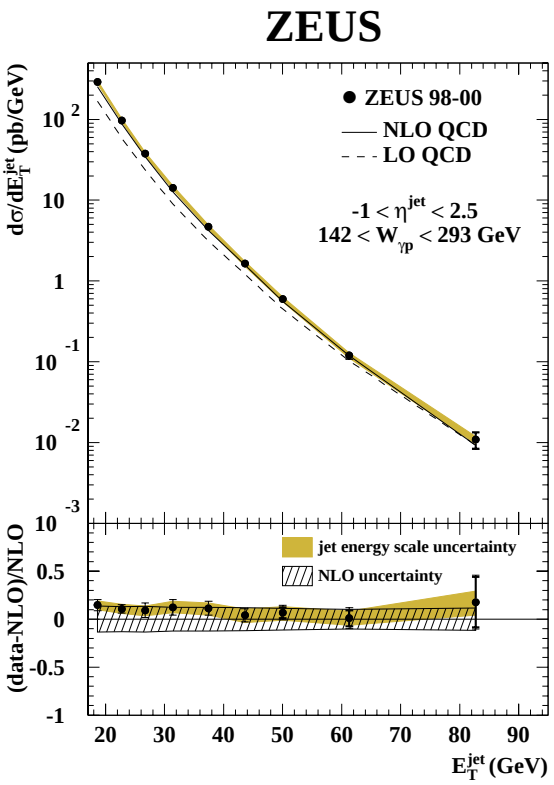

Fig. 18. Inclusive jet production in HEP ($Q^2 < 1$ Gev^2) integrated over $-1 < \eta_j < 2.5$. LO and NLO: Klasen, Kleinwort, Kramer with $\mu_R = \mu_F = E_{\rm T}$, proton-PDFs: MRST99, photon-PDFs: GRV

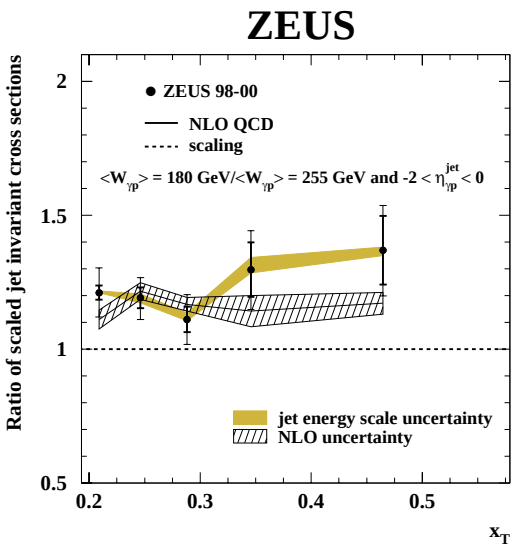

Fig. 19. Scaling violation in HEP ($Q^2 < 1$ GeV^2): Ratio of measured scaled invariant jet cross sections (see text) for the two $< W_{\gamma p} >$ shown and averaged over $-2 < \eta_j^{\gamma p} < 0$. NLO QCD as in Fig. 18

MRST99 with their corresponding $\alpha_s(M_Z)$-values. By combining the α_s values for different $E_{\rm T}$ bins, the value of $\alpha_s = 0.1224 +/- 0.0002(\text{stat}) + 0.0022/-0.0019(\text{exp}) + 0.0054/-0.0019(\text{theor})$ was obtained. The major error sources are the jet energy scale ($+/-1.5$ % in $\alpha_s(M_Z)$) and the renormalization scale ($+4.2/-3.3\%$ in $\alpha_s(M_Z)$); the uncertainties from the PDPs and hadronization are estimated to be less than 1%.

The energy scale dependence of α_s was investigated by determining α_s from $d\sigma/dE_{\rm T}$ at different $E_{\rm T}$ values. Thus, $d\sigma/dE_{\rm T}$ was parametrized in terms of $\alpha_s(\langle E_{\rm T}\rangle)$, where $\langle E_{\rm T}\rangle$ is the weighted mean of $E_{\rm T}$ in each bin. The resulting $\alpha_s(E_{\rm T})$ values (comp. Fig. 22) agree well with the predicted running of α_s.

Using the above data, ZEUS has measured the dependence of the scaled invariant jet cross sections $E_{{\rm T}j}^4 E_j d^3\sigma/dp_{xj}dp_{yj}dp_{zj}$ on the dimensionless variable $x_{\rm T} = 2E_{{\rm T}j}/W_{\gamma p}$. The cross section measured at $\langle W_{\gamma p}\rangle$ of 180 and 255 GeV and averaged over $-2 < \eta_j^{\gamma p} < 0$, agrees well with NLO QCD. In the quark parton model, the scaled cross section should be independent of $W_{\gamma p}$, whereas from QCD, one expects a violation of scaling due to the evolution of the structure functions and the running of α_s. As shown in Fig. 19, the ratio of the scaled cross section at the two different energies $W_{\gamma p}$ violates scaling as predicted by NLO QCD.

2.2. Inclusive Dijets

Dijet production has been studied by ZEUS [15] and H1 [16] under very similar kinematical conditions as in single jet production. In both experiments, the jets were reconstructed with ILICA requiring asymmetric cuts on $E_{\rm T}$ in the lab frame in order to avoid infrared unsafe regions of the phase space. Both experiments cover a range of $-1 < \eta_{j1,2} < 2.5$ and $0.1 < y < 0.9$. The quantity $x_\gamma^{\rm obs}$ is introduced as

$$x_\gamma^{\rm obs} = (E_{{\rm T}j1}e^{-\eta_1} + E_{{\rm T}j2}e^{-\eta_2})/2yE_e, \qquad (5)$$

where $y = W^2/s$ and which corresponds in LO to the fraction of the photon momentum that contributes to the production of the two highest $E_{\rm T}$ jets; cuts on $x_\gamma^{\rm obs}$ allow one to enrich the data with direct processes (high x) or resolved processes (low x). The measurements are compared to the NLO QCD calculations in which $\mu_R = \mu_F$ is set to the average $E_{\rm T}$ of the two outgoing partons. The PDF-parametrizations used are GRV-HO and AFG-HO for the photon and CTEQ5M1 for the proton; $\alpha_s(M_Z)$ is set to 0.118.

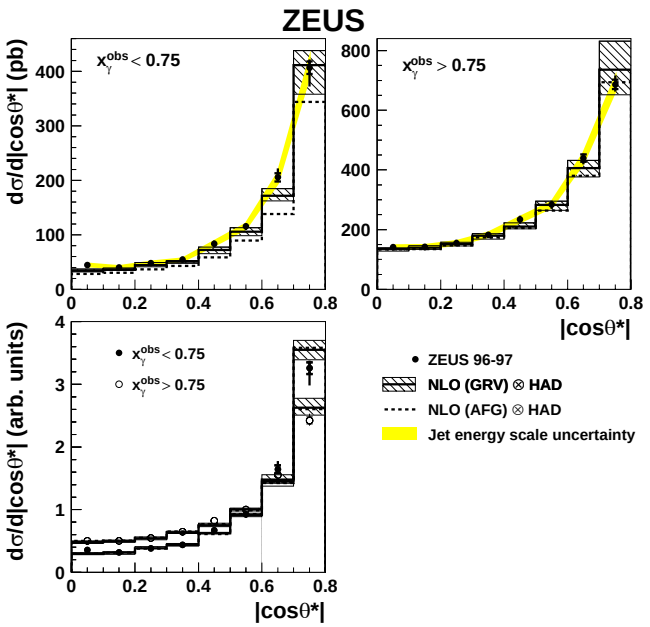

Fig. 20. Inclusive dijet production in HEP ($Q^2 < 1$ GeV^2) as a function of the dijet angle Θ^* in the parton-parton-cms for different cuts on the fractional momentum $x_\gamma^{\rm obs}$ of the photon participating in the production of the two jets with highest transverse energy. Cuts: $E_{{\rm T}j1,2} > 14, 11$ GeV; $-1 < \eta_j < 2.4; 134 < W_{\gamma p} < 277$ GeV. NLO: Frixione, Ridolfi with CTEQ5M for proton-PDFs and GRV resp. AFG for photon-PDFs

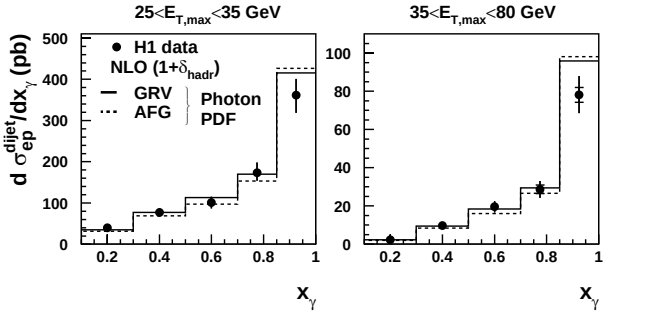

Fig. 21. Inclusive dijet prodution in HEP ($Q^2 < 1$ GeV^2) as a function of the fractional momentum x_γ of the photon participating in the production of the two jets with highest transverse energy $E_{\rm T}$ (identical with $x_\gamma^{\rm obs}$ in Fig. 20). Cuts: $E_{{\rm T}j1,2} > 25, 15$ GeV; $-0.5 < \eta_j < 2.5$; $95 < W_{\gamma p} < 285$ GeV. QCD, PDFs as in Fig. 20

The measured angular distributions of the dijet cross section (Fig. 20) confirm the steeper rise expected for resolved photon processes ($x_\gamma^{\rm obs} < 0.75$) in comparison to direct photon processes ($x_\gamma^{\rm obs} > 0.75$), indicating that the dynamics of the hard scattering process is well understood. For the H1 data, the cross section as a

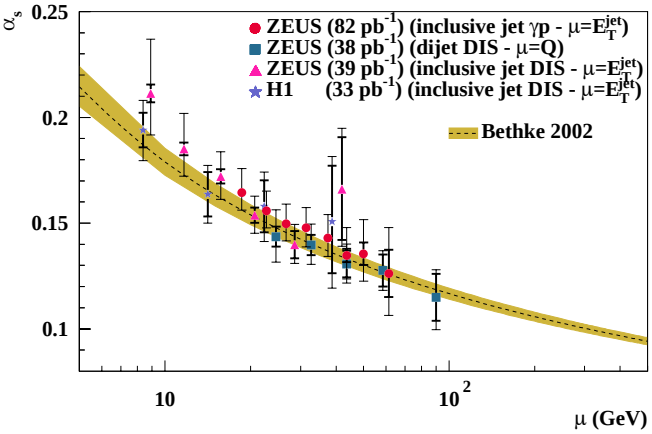

Fig. 22. Scale dependence of α_s from recent HERA experiments

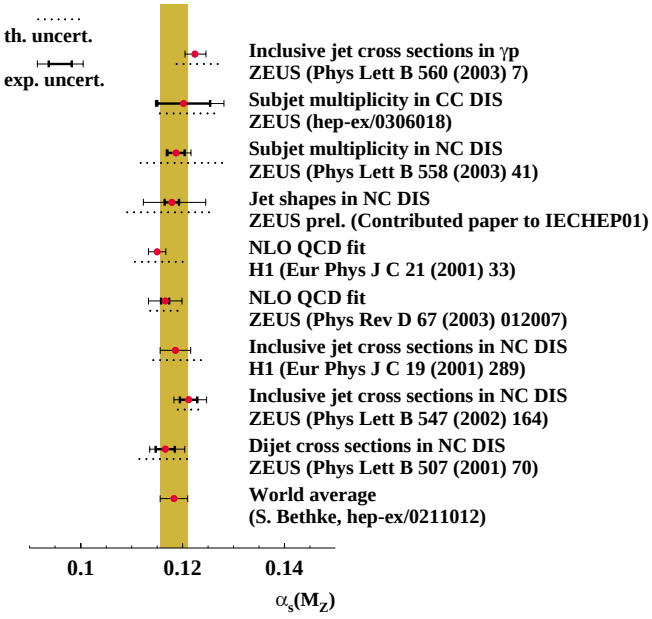

Fig. 23. Determination of $\alpha_s(M_Z)$ and its scale dependence in recent HERA experiments

function of x_γ (which is identical with $x_\gamma^{\rm obs}$), shown in Fig. 21 for two regions of $E_{\rm T,max}$ representing two different factorization scales for the PDFs of the proton and photon, agrees reasonably well with NLO predictions and varies slightly only with the different parametrizations of the photon PDFs while ZEUS observes differences. It has to be noted, however, that this discrepancy might be due to the different $E_{\rm T}$-cuts in the measurements; while H1 uses $E_{\rm T1} > 25$ GeV, $E_{\rm T2} > 15$ GeV, ZEUS uses $E_{\rm T1} > 14$ GeV, $E_{\rm T2} > 11$ GeV.

3. Summary of Results on α_s

The results obtained from the recent measurements of jet and subjet cross sections in DIS and HEP on $\alpha_s(M_Z)$ as well as on the scaling behaviour of α_s have achieved an accuracy well compatible with results from other colliders. They are also in good agreement with the world average (Fig. 22 and 23).

Summary

For large scales, Q^2 and/or jet E_{T}, the recent results from H1 and ZEUS on jet production in deep inelastic scattering and high energy photoproduction are in good agreement with NLO QCD. In general, the hadronization corrections applied to the NLO results are small and improve the description of the data only slightly. For decreasing scales and in specific areas of phase space, the corrections may become large and are important in improving the description of the data.

In these studies, the longitudinally invariant k_T cluster algorithm in its inclusive mode has proved reliable and, therefore, become the preferred method of jet identification in this high energy region. The good agreement of α_s determinations performed with jet (and subjet) production at high Q^2 and E_{T} with the world average supports this conclusion.

The situation is worse in the small x / forward region. For $x < 10^{-4}$ and small Q^2, a breakdown of DGLAP is to be expected and indeed increasing discrepancies with DGLAP based predictions are observed even in NLO. In some cases in spite of small experimental errors, the sizable theoretical uncertainties, however, do not yet allow safe conclusions on a more satisfactory and comprehensive description of the data by modified pQCD models like BFKL or CCFM.

Not only an improvement of experimental statistical and systematic errors to come from HERA II, but also more accurate model calculations are needed to get closer to a satisfactory understanding of the interplay of soft and hard QCD processes in DIS and HEP.

I am indebted to Günter Grindhammer for his critical reading of the paper and many valuable comments and to Kristiane Preuss and Marlene Schaber for their help in the preparation of the talk and the paper. My thanks are due to P.N. Bogolyubov and L. Jenkovsky for the invitation to an interesting and enjoyable conference.

1. *Adloff C. et al.* // Europ. Phys. J. – 2001. – **C19**. – P. 289. – DESY 00-145; hep-ex/0010054.
2. *Chekanov S. et al.*// Phys. Lett. – 2002. – **B547**. – P. 164. – DESY 02-112; hep-ex/0208037.
3. *Chekanov S. et al.*// Ibid. – 2003. – **B551**. – P. 226. – DESY 02-171; hep-ex/0210064.
4. *Adloff C. et al.*// Ibid. – 2002. – **B542**. – P. 193. – DESY 02-079; hep-ex/0206029.
5. *Jung J.*// H1 Collaboration, ICHEP 02. – Amsterdam, 2002.
6. *Goerlich L.*// H1 Collaboration. – DIS 2003. – St. Petersburg, 2003.
7. *Lammers S.*// ZEUS Collaboration. – DIS 2003. – St. Petersburg, 2003.
8. *Breitweg J. et al.*// Phys. Lett. – 2001. – **B507**. – P. 70. – DESY 01-018; hep-ex/0102042; *Chekanov S. et al.*// Europ. Phys. J. – 2002. – **C23**. – 13. – DESY 01-127; hep-ex/0109029.
9. *Poeschl R.*// H1 Collaboration. – DIS 2003. – St. Petersburg, 2003.
10. *Adloff C. et al.*// Phys. Lett. – 2001. – **B515**. – P. 17. – DESY 01-073; hep-ex/0106078.
11. *Krumnack N.*// ZEUS Collaboration. – DIS 2003. – St. Petersburg, 2003.
12. *Chekanov S. et al.*// Phys. Lett. – 2003. – **B558**. – P. 41. – DESY 02-217; hep-ex/0212030.
13. *Adloff C. et al.* (submitted to Europ. Phys. J. – **C**. – DESY 02-225); hep-ex/0302034.
14. *Chekanov S. et al.*// Phys. Lett. – 2003. – **B560**. – P. 7. – DESY 02-228; hep-ex/0212064.
15. *Chekanov S. et al.*// Europ. Phys. J. – 2002. - **C23**. – P. 61.– DESY 01-220; hep-ex/0112029.
16. *Adloff C. et al.*// Ibid. – **C25**. – P. 13. – DESY 01-225; hep-ex/0201006.

ВИВЧЕННЯ СТРУМЕНІВ ТА α_s-ВИМІРЮВАННЯ НА ПРИСКОРЮВАЧІ HERA

Г.В. Бушхорн

Р е з ю м е

Викладено недавні результати, отримані H1- і ZEUS-колаборацiями на прискорювачі HERA, з інклюзивного народження одиничних та множинних струменів в глибоконепружному розсіянні електронів/позитронів на протонах, що визначається нейтральним струмом, а також з високоенергетичного фотонародження на протонах. Коротко описано методи аналізу струй, а експериментальні результати порівняно з НВП КХД-розрахунками. Обговорюються способи визначення константи зв'язку сильної взаємодії α_s, що випливають з цих вимірювань струменів.

ИЗУЧЕНИЕ СТРУЙ И α_s-ИЗМЕРЕНИЯ НА УСКОРИТЕЛЕ HERA

Г.В. Бушхорн

Р е з ю м е

Представлены недавние результаты, полученные H1- и ZEUS-коллаборациями на ускорителе HERA, по инклюзивному рождению единичных и множественных струй в глубоконеупругом рассеянии электронов/позитронов на протонах, определяемом нейтральным током, а также по высокоэнергетическому фоторождению на протонах. Кратко описаны методы анализа струй, а экспериментальные результаты сравниваются с СЛП КХД-вычислениями. Обсуждаются способы определения константы связи сильного взаимодействия α_s на основе этих измерений струй.